

The K-band Spectrum of The Hot Star in IRS 8: An Outsider in the Galactic Center?¹

T. R. Geballe², F. Najarro³, F. Rigaut², J.-R. Roy²

ABSTRACT

Using adaptive optics at the Gemini North telescope we have obtained a K-band spectrum of the star near the center of the luminous Galactic center bowshock IRS 8, as well as a spectrum of the bowshock itself. The stellar spectrum contains emission and absorption lines characteristic of an O5-O6 giant or supergiant. The wind from such a star is fully capable of producing the observed bowshock. However, both the early spectral type and the apparently young age of the star, if it is single, mark it as unique among hot stars within one parsec of the center.

Subject headings: shock waves – stars: winds, outflows – Galaxy: center – infrared: ISM, stars

1. Introduction

The nature of the Galactic center source IRS 8 (Becklin & Neugebauer 1975), one of the brightest compact mid-infrared sources in the central infrared cluster, was unknown until adaptive optics H- and K-band imaging revealed that the bulk of its infrared emission originates in a classic bowshock (Rigaut et al. 2003; Geballe et al. 2004). Geballe et al. (2004) showed that the IRS 8 bowshock is a straightforward consequence of the interaction of a dense

¹Based on data obtained at the Gemini Observatory, which is operated by the Association of Universities for Research in Astronomy, Inc., under a cooperative agreement with the NSF on behalf of the Gemini partnership: the National Science Foundation (United States), the Particle Physics and Astronomy Research Council (United Kingdom), the National Research Council (Canada), CONICYT (Chile), the Australian Research Council (Australia), CNPq (Brazil) and CONICET (Argentina).

²Gemini Observatory, 670 N. A'ohoku Place, Hilo, Hawaii 96720 USA; tgeballe@gemini.edu

³Instituto de Estructura de la Materia, CSIC, Serrano 121, 29006 Madrid, Spain

and high velocity wind from a hot star that is traversing moderately dense interstellar gas. Adaptive optics imaging on large telescopes easily resolves the central star of IRS 8 (hereafter IRS 8*) from the bowshock.

That stars undergoing mass loss within the interstellar medium in the Galactic center produce bowshock-like structures of swept-up gas had already been suggested from observations of IRS 21 by Tanner et al. (2002) and, by analogy, for a number of other luminous mid-infrared sources in the Northern Arm. This has now been observationally verified (Tanner et al. 2005) and additional examples of the phenomenon have been found (Genzel et al. 2003; Clénet et al. 2004a,b). Thus IRS 8 is the most graphic example of a common phenomenon in the Galactic center that may also include a large number of lower luminosity sources with less massive winds (e.g., Eckart et al. 2004).

Because of its large angular dimensions, fortuitous orientation, and relatively isolated location, spectroscopy of IRS 8 at high angular resolution can provide information both on the nature of the stellar source of the wind and the properties of the wind and the interstellar medium in the Galactic center. Here we describe exploratory low resolution K-band spectroscopy of IRS 8* and its bowshock.

2. Observations and Data Reduction

K-band spectra of IRS 8 were obtained on UT 2004 June 9 and 2005 August 21 at the Frederick Gillett Gemini telescope on Mauna Kea, in photometric conditions. The Gemini adaptive optics module ALTAIR was used to feed NIRI, the facility near-infrared imager and spectrograph, with a near-diffraction limited view of the IRS 8 region. The adaptive optics correction was performed on a $V \sim 14$ mag star $13''$ distant from IRS 8*. NIRI was configured with a $0.10''$ slit and a K grism to cover the $1.9\text{--}2.4 \mu\text{m}$ wavelength interval with resolving power of 900. The plate scale was $0.0219'' \text{ pixel}^{-1}$. Exposures were obtained with IRS 8* alternately positioned at two locations along the slit, separated by $3''$. The slit was oriented east-west on the sky and thus intersected the bow shock a few tenths of an arcsecond south-southeast of its apex, as shown in Fig. 1.

Spectra of both IRS 8* (covering 6 rows of the array) and the bow shock (covering 7 rows of the array centered $0.24''$ east of the star) were extracted from the best quality subtracted pairs of flatfielded and despiked spectral images, and were then coadded to produce final raw spectra. Only the 2005 data consisting of 30 minutes of exposure time are shown here. In the initial data reduction the spectra of IRS 8* and the bowshock were ratioed by the spectrum of HR 7038 (F5V, observed immediately after IRS 8), following artificial removal

(via interpolation) of the Br γ line in its extracted spectrum. Prior to ratioing a slight smoothing was applied to all coadded spectra, resulting in a final resolving power of 870, corresponding to a velocity resolution of 350 km s^{-1} . The wavelength scale was calibrated using telluric absorption lines in the spectrum of HR 7038, and is accurate to $0.0003 \mu\text{m}$ (40 km s^{-1} , 2σ).

Examination of the intensity profile of the spectral images along the slit indicated that contamination by the spectrum of the surrounding bowshock contributed significantly to the spectrum of IRS 8*, e.g., 25 ± 5 percent at $2.2 \mu\text{m}$. This contamination was subtracted from the IRS 8* spectrum to produce the final spectrum. As the spectrum of the bowshock is smooth in the vicinity of almost all of the lines reported below in IRS 8*, and because the bowshock is both fainter than IRS 8* at all but the longest wavelengths in the spectrum and percentage-wise a minor contaminant, the above uncertainty in the percentage of the bowshock spectrum to be subtracted has a negligible effect on the strengths of these lines and results in only a small increase in the noise level.

Figure 2 contains the reduced spectra of both the star and the bowshock. Cancellation of the strong telluric band of CO_2 near $2.01 \mu\text{m}$ was poor and thus that portion of the spectra is omitted in the figure. In addition, as can be seen by the similar structures near the long wavelength ends of the two spectra, accuracy in the $2.27\text{-}2.33 \mu\text{m}$ regions of the spectra is limited by systematic errors in telluric line removal. Over the bulk of each spectrum, however, the fluctuations appears to be random.

The spectrum of the bowshock is a steeply rising continuum with weak and narrow He I singlet and H I Br γ emission lines present near $2.059 \mu\text{m}$ and $2.166 \mu\text{m}$, respectively. The spectrum of the central star has a considerably less steep continuum and clearly contains several weak emission lines in the $2.07\text{-}2.12 \mu\text{m}$ interval, but neither of the emission lines seen in the bowshock.

A more careful data reduction of the spectrum of IRS 8* was performed by dividing the spectrum as before by the standard with the straight line interpolation at Br γ , but then multiplying by the normalized F5V standard spectrum from Wallace & Hinkle (1997) at all wavelengths except in the Br γ region prior to decontamination. By doing this subtle emission features in the reduced spectrum resulting from weak absorption lines in HR 7038 are removed. Because the strong Br γ lines in HR 7038 and in the template do not quite match, we have used a straight line interpolation there. The spectrum resulting from this reduction method is used in the remainder of this paper.

From Scoville et al. (2003) the extinction in the general vicinity of IRS 8 is $A_V \sim 28$ mag. When the spectrum of IRS 8* is dereddened by this amount the continuum is noticeably

redder than the Rayleigh-Jeans spectral falloff of a hot star. Thus either the fully reduced and dereddened stellar spectrum is still considerably contaminated by emission from dust (despite our removal of contamination as described previously) or the extinction to IRS 8* is somewhat larger than the value inferred from the extinction map of Scoville et al. (2003). We suspect the latter and that fine spatial structure in the extinction is the most likely cause of the discrepancy. To estimate the extinction at IRS 8* we compared the dereddened stellar spectral energy distribution (SED) with those from our theoretical models of the IRS 8* spectrum (see below). The best match was obtained for a value of $A_V=33$ mag. Values differing from this by >1.5 mag failed to reasonably reproduce the observed slope of the SED. From our estimate of $K=13.3$ for IRS 8* based on these data¹ we obtain a dereddened $K=9.50$ mag or $M_k=-5.0$ mag for an assumed distance of 8 kpc to the Galactic center.

The reduced and dereddened 2.04-2.27 μm spectrum of IRS 8* is shown in Fig. 3. The signal-to-noise ratio, estimated from the fluctuations in lineless parts of the spectrum, varies with wavelength but is never far from 100 in a resolution element ($\sim 0.0025 \mu\text{m}$); it is highest from 2.21 to 2.27 μm . The narrow emission features near 2.1 μm have peaks at 2.070 μm , 2.080 μm , 2.106 μm , and 2.116 μm . These features are respectively identified as: C IV (2.0705 μm ; C IV 2.0796 μm); a blend of nearly coincident C III and N III lines at 2.1038 μm and 2.1081 μm ; and nearly coincident C III, N III and O III contributions at 2.1152 μm , 2.1155 μm , 2.1156 μm and 2.1162-69 μm (Najarro 1995; Hanson, Conti, & Rieke 1996). All wavelengths are *in vacuo*. The He I lines at 2.1126 μm and 2.1138 μm are very weak and embedded within the emission feature at 2.116 μm (see discussion below). An additional weak but statistically significant emission feature is present at 2.247 μm and is identified as the stronger and shorter wavelength member of an N III doublet that has previously been seen in late WN stars (Figer, McLean, & Najarro 1997; Najarro et al. 2004) and perhaps is also weakly present in the O stars observed by Najarro et al. (2004). The statistically significant absorption feature at 2.190 μm is He II 10-7. The He I 2¹P-2¹S line is weakly in absorption at 2.059 μm . All of these features except for the last are also clearly detected in the spectrum of IRS 8* obtained in 2004 June. The Br γ line is not detected and its integrated equivalent width must be very small.

¹We note the significant difference between the current K magnitude and the one derived from photometry by Geballe et al. (2004), but use the present value because of considerably improved performance of the Gemini adaptive optics system since the previous measurement and because nothing is known about the variability of IRS 8*.

3. Discussion

3.1. Radial velocities

At the location of IRS 8 Lacy, Achtermann, & Serabyn (1991) identified two velocity components in the Ne II line at $12.8 \mu\text{m}$, one at -10 km s^{-1} which is localized at IRS 8 and the other centered near $+110 \text{ km s}^{-1}$ associated with the Northern Arm. The signal-to-noise ratios of the lines in the IRS 8* spectrum are not high and the resolving power is low; hence the radial velocities of the lines cannot be determined accurately. Nevertheless, we can draw some limited conclusions from our model fits (see section 3.3) to the observed spectrum. Fits to the $2.07\text{-}2.12 \mu\text{m}$ complex of lines gives -10 km s^{-1} . Fits to the He absorption lines give $+30 \text{ km s}^{-1}$. The mean value of these is $+10 \text{ km s}^{-1}$. The strong Br γ line in the bowshock is centered at -40 km s^{-1} . All of these values match the radial velocity of the more negative component of the Ne II line to within the uncertainties. We thus conclude that the blueshifted Ne II component seen by Lacy, Achtermann, & Serabyn (1991) is associated with IRS 8* and suspect that it arises in gas that has been swept up by the wind from IRS 8*. Apparently, the Northern Arm is not interacting with IRS 8 and thus IRS 8* lies either well in front of it or behind it.

3.2. Classification of IRS 8*

The relatively small equivalent widths of the emission lines in the spectrum of IRS 8* indicate that the star is an OB type rather than a Wolf-Rayet type. A very few WC9 stars with weak $2 \mu\text{m}$ lines have been found by Figer, McLean, & Najarro (1997); however, the lines are considerably broader than observed here. The isolated C IV lines in IRS 8* have widths that are only marginally broader than the velocity resolution of 350 km s^{-1} , indicating that the intrinsic full widths at half maximum (FWHMs) of the lines are not larger than 200 km s^{-1} , consistent with rotational velocities found for O stars with lines originating at the photosphere. The presence of the two helium lines in absorption suggests that the star is either an Of or WNL type (Hanson, Conti, & Rieke 1996; Figer, McLean, & Najarro 1997), but the latter classification is unrealistic as the carbon lines at $2.07 \mu\text{m}$ and $2.08 \mu\text{m}$ are prominent. Thus we are confident that we are observing an O star.

Hanson, Conti, & Rieke (1996), and Hanson et al. (2005) have developed an infrared classification scheme for OB stars, based on spectra in the H window and short wavelength half of the K window, which is useful for hot stars that suffer large extinctions. Figure 3 is a comparison of the IRS 8* K-band spectrum with online-available K-band spectra from the Hanson, Conti, & Rieke (1996) catalog for O stars ranging from O4 to O6.5 and different

luminosity classes. The resolving powers for all template spectra have been degraded to 800 for direct comparison with the observed spectrum.

From Fig. 3 we judge that IRS 8* falls within the O5-O6.5 and III-If ranges, with likely O5-O6 If spectral type and luminosity class. For stars earlier than O5-O6If the C III/N III lines become much weaker while the strengths of the C IV lines are considerably reduced for both earlier and later spectral types. In addition, in cooler stars He I usually begins to develop a noticeable absorption at 2.113 μm (see Hanson, Conti, & Rieke (1996) for further objects with later spectral type), but this line is not detected in IRS 8*. A similar trend is observed in the He I line at 2.059 μm line, as its absorption strength clearly increases toward later types. Two spectral features may be used to determine the luminosity class: the emission feature at 2.116 μm and Br γ . From Fig. 3 we see that for a given spectral type the emission strength of the 2.116 μm feature is larger for supergiants than for dwarfs. Also emission in the strong stellar winds present in the supergiants starts to fill the Br γ photospheric absorption profile to drive this line into emission as opposed to the clean absorption profile observed for giants and dwarfs.

Further constraints on the spectral type of IRS 8* might come from measurements of the ionization state of the surrounding gas using mid-infrared fine structure lines of ions with a diagnostic range of ionization potentials. Lacy et al. (1980) found from observations of the Ne II, Ar III, and S IV lines that the overall ionization state in the central parsec of the Galaxy is consistent with excitation by stars with $T_{eff} \leq 35,000$ K. If that constraint applies to IRS 8 the earlier O spectral subtypes in the above range could be ruled out. The Ne II line intensity at IRS 8 has been measured and is strong, but searches for the Ar III and S IV lines at IRS 8 have not been reported.

3.3. Stellar parameters and abundances

Given the strong spectral similarities of IRS 8* with the O5-6 supergiants in Cyg OB2 (see Fig. 3), we computed model fits covering that parameter domain, drawing from our analysis of the Cyg OB2 stars for which UV, optical and IR spectra are available (Herrero, Puls & Najarro 2002, Najarro et al. in preparation). To perform quantitative analysis we utilized the iterative, non-LTE line blanketing method presented by Hillier & Miller (1998) and proceeded as described in Najarro et al. (2004), also taking into account the effects of the Fe IV lines close to the wavelength of the He I 2.06 μm line (Najarro et al. 2006). The reader is referred to Hillier & Miller (1998) and Hillier & Miller (1999) for a detailed discussion of the code. Our best-fitting model is displayed in Fig. 3 (dashed line) and reproduces the observed K-band spectrum of IRS 8* quite well. Although the observed K band flux and

low resolution spectrum are insufficient to tightly constrain all of the stellar properties of a supergiant such as IRS 8* (higher resolution and other H lines would be required), it is possible to obtain accurate estimates of some crucial parameters such as temperature and luminosity and useful constraints on the wind density and metal abundances.

To determine the effective temperature we use He I/II ionization balance as the main constraint via the He I 2.06 and 2.112/3 μm lines and the He II 2.189 μm line. The C IV lines are considered as secondary T_{eff} indicators (see below). The strengths of the absorption components of neutral helium lines display the highest sensitivity to changes in temperature, while the He II 2.189 μm line also shows strong sensitivity to wind density (\dot{M}). Within the parameter domain of interest, for reasonable He enrichment (e.g. He/H < 0.25 by number), these lines are not highly sensitive to changes in He abundance if the mass loss rate is also adjusted to reproduce Br γ . This may be understood as follows. When the He abundance increases, the He absorption lines become somewhat stronger. However, to recover the observed Br γ strength \dot{M} must be increased to compensate for the reduction in the hydrogen abundance. The higher mass loss rate refills the He absorption components and, therefore, the resulting He profiles do not change significantly. This situation is reversed when the He abundance is high enough (He/H > 0.25 by number) as both effects, enhancement of He abundance and increased \dot{M} , drive the He lines into emission. From the above, we obtain $T_{eff}=36000 \pm 2000$, $\log L/L_{\odot} = 5.6 \pm 0.2$ (set by the derived T_{eff} and the observed K magnitude), and $0.10 < \text{He}/\text{H} < 0.25$ by number.

The error estimate for the effective temperature may seem small, but we are confident of the robustness of the derived value given the strong sensitivity of the He I absorption components and the He II line together with the presence of the C IV lines. For temperatures above 38000 K the He I lines absorption components disappear while they clearly become too strong for effective temperatures below 34000 K. Likewise, the He II line starts to fade for temperatures below our quoted range and gets too strong in absorption for temperatures above it. Is also important to note that, for the relevant parameter domain, the He I/II lines react only minorly to changes on the surface gravity. The error in the stellar luminosity reflects those in the effective temperature, extinction, contribution of the bow-shock spectrum and the uncertainty in the flux calibration.

The Br γ line is strongly sensitive to wind density, clumping, and velocity field, and to a lesser extent to gravity. Since we do not have diagnostics for the terminal velocity to constrain the wind density, we adopt a typical value, 2500 km s⁻¹, found for other galactic O5If stars (Herrero, Puls & Najarro 2002). Further, the spectral resolution is not high enough to clearly constrain either the shape of the velocity field (e.g., the β parameter Najarro et al. 2004) or the clumping factor (f). Thus, depending on the adopted β and He abundance we obtained

clumping scaled mass loss rates \dot{M}/\sqrt{f} in the range $4.5\text{--}6.2 \times 10^{-6} M_{\odot} \text{ yr}^{-1}$. For our models we assumed a clumping factor of $f=0.15$, based on our experience of modeling the Cyg OB2 objects, and hence the resulting mass-loss rates ranged from 1.75 to $2.45 \times 10^{-6} M_{\odot} \text{ yr}^{-1}$ for the adopted β and terminal velocity. Likewise, the lack of cleaner diagnostic lines for gravity such as the Brackett series lines in the H-band, hampers the determination of $\log g$. Models with gravities above $\log g=3.70$ started to fail to reproduce the spectrum. Reasonable fits were obtained for models with $\log g=3.40\text{--}3.60$.

The C IV lines were utilized as a secondary temperature diagnostic (see also Lenorzer et al. 2004), as they not only depend quite strongly on temperature, but also on wind density, carbon abundance, gravity and the β parameter. If none of the above parameters are precisely determined, the uncertainty in the carbon abundance may be as high as a factor of three. In the case of IRS 8* currently acceptable values for the carbon abundance range from $0.25 \times$ solar to $0.6 \times$ solar.

The N III doublet at $2.25 \mu\text{m}$ reacts mainly to nitrogen abundance and only slightly to effective temperature within the parameter domain of interest and thus constitutes an excellent diagnostic of the nitrogen abundance (see also Najarro et al. 2004). However, the weakness of this feature relative to the noise level results in a relatively high uncertainty in the lower limit to the nitrogen abundance. We estimate an enrichment of roughly $5 \times$ solar with $7.5 \times$ solar and $2.5 \times$ solar as reasonable upper and lower limits respectively.

The strong emission feature at $2.116 \mu\text{m}$ in IRS 8* is of particular interest. In the past this feature, which is present over a very wide range of O spectral types and luminosities (Hanson, Conti, & Rieke 1996) has been attributed to C III and N III $n=8\text{--}7$ transitions. We tried to reproduce this feature with the carbon and nitrogen abundances derived from the C IV $2.07\text{--}2.08 \mu\text{m}$ and N III $2.25 \mu\text{m}$ lines and missed more than half of the observed equivalent width of the feature. Increasing either the carbon or the nitrogen abundance to match the $2.116 \mu\text{m}$ feature resulted in far too strong lines of C IV at $2.07\text{--}2.08 \mu\text{m}$ and/or N III at $2.25 \mu\text{m}$. This result is confirmed by inspection of the dominant ions of these species within the atmospheric region where the above lines form. Carbon is largely divide between C IV and C V, so the C III lines are too weak even with a large increase in the carbon abundance. The dominant ions of nitrogen and oxygen are N IV and O IV and hence the N III and O III recombination lines are reliable diagnostics for deriving abundances. Hence, we now believe that the $2.116 \mu\text{m}$ feature in IRS 8* is dominated by O III $n=8\text{--}7$ transitions. After extending our O III model atom to account for these transitions we could satisfactorily reproduce the observations (see Fig. 3). Further, the O III component of the $2.116 \mu\text{m}$ feature largely depends on the oxygen abundance and only slightly on gravity, effective temperature, wind density, and velocity field. Thus, this feature may be a powerful

diagnostic of oxygen abundance, and therefore an important metal abundance determiner, over a wide range of O spectral types (Najarro et al. in preparation). Using it we obtain an oxygen abundance of 0.8 to $1.1 \times$ solar in IRS 8*, which indicates solar metallicity for the cloud in which IRS 8* formed.

To summarize this subsection, the stellar parameters T_{eff} , L , \dot{M}/\sqrt{f} , and $\log g$ are fully compatible with OIf supergiants (e.g. Herrero, Puls & Najarro 2002) and confirm the nature of IRS 8* derived from classification schemes. The derived N/C and N/O ratios reveal partial CNO processing at the surface of IRS 8 and are consistent with the values expected for an O supergiant if rotational mixing has taken place.

Geballe et al. (2004) used the measured standoff distance of the bowshock from the star together with a rough estimate of the particle density ($n = 10^3 \text{ cm}^{-3}$) of the ambient interstellar medium in the Galactic center and typical values of windspeed (10^3 km s^{-1} and mass loss rate in a hot star ($10^{-6} M_{\odot} \text{ yr}^{-1}$) to estimate a space velocity v_* for IRS 8* of 150 km s^{-1} , which is a reasonable value in the Galactic center. The standoff distance is proportional to $(\dot{M} v_w / n v_*^2)^{0.5}$, where \dot{M} is the mass loss rate and v_w is the wind speed. The values of v_w and \dot{M} used in the above modelling suggest that in order to produce the observed standoff distance n would need to approach 10^4 cm^{-3} , which would not be surprising.

3.4. Evolutionary status and mass of IRS 8*: An outsider within the Galactic center context?

Recently, Paumard et al. (2006) have reported the spectroscopic identification of ~ 40 OB supergiants, giants and dwarfs in the central parsec of the galaxy. Interestingly they find no OB stars outside the inner 0.5 pc (radius) of the galaxy and the earliest spectral type in their OB sample lies around O8-9I. They derive a common age of $6 \pm 2 \text{ Myr}$ for the cluster.

Our analysis suggests that IRS 8*, although only 1 pc from the center, does not fit into this picture of the central cluster of hot stars. It is of much earlier spectral type than any of the stars classified by Paumard et al. (2006). Currently it is the only known OB star outside the central 0.5 pc region of the cluster. Figure 4 shows the position of IRS 8* (solid cross) as estimated from our model fits in the HR diagram compared with different evolutionary scenarios. An estimate of the evolutionary status of IRS 8*, based on comparisons with evolutionary tracks of stars without rotation (e.g. Maeder & Meynet 2003, not displayed in Fig. 4) yields a star with a zero age main sequence (ZAMS) mass of $48 M_{\odot}$ and a current age of 2.8 Myr. Such a star would not show any processed material on its surface. This is clearly

at odds both with the current estimate for the age of the Galactic center cluster and with the abundance pattern derived from our models. The situation improves when evolutionary models accounting for rotation (dashed-lines in Fig. 4) are considered (Maeder & Meynet 2003). Then the current position in the HR diagram corresponds to a star with a ZAMS mass of $44.5 M_{\odot}$ and an age of 3.5 Myr. Such a star would show CNO-processed material on its surface. Except for the age, still well below the estimate obtained by Paumard et al. (2006) using non-rotating models for a single burst scenario, the stellar parameters, including the abundance pattern, are fully consistent with those derived from our modelling.

The crucial question thus is whether this star is really much younger than the cluster and probes the existence of ongoing (or at least much more recent) star formation, or if on the contrary the star is either an impostor or a cluster member that underwent a rejuvenation cure. A possible way out is provided if the star originally was a member of a massive close binary system. In such a case, we could be looking now at the secondary star, with the primary either exploded as supernova or in an evolutionary phase when it is much dimmer at K than the secondary. Models for massive close binaries have been developed by Wellstein & Langer (1999) to explain the optical counterparts of massive X-ray binaries. Using these models we have found that for a massive close binary system with initial masses of $25 M_{\odot}$ and $24 M_{\odot}$ (their model 10a) the current position of IRS 8* may be elegantly explained without violating the age of the Galactic center cluster. Similar scenarios are a possible explanation for some of the overluminous He I objects in the central parsec. The solid lines in Fig. 4 correspond to the evolution of the primary (grey) and secondary (black) components of the massive close binary system. The thick solid line displayed on the track of the secondary corresponds to the phase where the primary is at least 10 times less bright in K than the secondary. The observed location of IRS 8* in the HR diagram is reached after 7.1 Myrs, which is consistent with the 6 ± 2 Myr estimate from Paumard et al. (2006). Furthermore, at this stage the surface enrichment displayed by the secondary shows excellent agreement with the values derived in our model. For this particular massive close binary model the primary has not exploded yet, as otherwise the secondary would be already halfway through core helium burning and would have a much lower effective temperature. However, models with a slightly more massive primary and a slightly less massive secondary (N. Langer, private communication) could also reproduce the elemental abundances and current position of IRS 8* in the HR diagram after the explosion of the primary (at ~ 6 Myr) and, in addition, could have provided a kick to the secondary, placing it at its current position outside the central 0.5 pc.

The spectroscopic mass of IRS 8* is in the range $23\text{--}37 M_{\odot}$ (for $\log g$ 3.40–3.60), although the range could be larger, bearing in mind the uncertainties in determining the stellar gravity, as discussed previously. From the evolutionary models of (Maeder & Meynet 2003), the

current mass of IRS 8* is $38 M_{\odot}$ for a single star evolution with rotation, and thus consistent with the highest values of spectroscopic mass. Likewise, in the close binary scenario, the current mass of IRS 8* (after consuming a significant fraction of its companion) is $36\text{--}40 M_{\odot}$.

Future spectra at higher resolution than presented here should be able to test if IRS 8* is part of a close binary. If IRS 8* is single its origin is highly uncertain. It is then either an impostor in the central parsec or it is a loosely associated member of the central cluster of hot and massive stars. The current motion of IRS 8*, nearly directly away from the center (as judged by the orientation of the bowshock and low radial velocity), suggests that it passes close to Sgr A* (Geballe et al. 2004) and may once have been a member of central cluster. If so it might be that a small population of less evolved and less luminous mid-late O type stars with weak emission lines such as those of IRS 8* are still hidden within the cluster, which could challenge the current understanding of that cluster as having a common age (Paumard et al. 2006).

We thank the staff of the Gemini Observatory for its support of these observations, which were performed as part of program GN-2004A-SV-203. We also thank the builders of the ALTAIR adaptive optics system at Gemini. F.N. acknowledges PNAYA2003-02785-E AYA2004-08271-C02-02 projects and the Ramon y Cajal program. We thank John Hillier for providing his atmospheric code. We also are indebted to Keith Butler for his advice on upgrading the model atoms and especially to Norbert Langer for fruitful discussions and providing the evolutionary tracks for massive close binaries. We are grateful for advice from Paul Crowther and Don Figer and for helpful comments from the referee.

REFERENCES

- Becklin, E. E. & Neugebauer, G. 1975, *ApJ*, 200, L71
- Clénet, Y., et al. 2004a, *A&A*, 417, L15
- Clénet, Y., et al. 2004b, *A&A*, 424, L21
- Eckart, A., Moulataka, J., Viehmann, T., Straubmeier, C., & Mouawad, N. 2004, *ApJ*, 602, 760
- Figer, D. F., et al. 2002, *ApJ*, 581, 258
- Figer, D. F., McLean, I. S., & Najarro, F. 1997, *ApJ*, 486, 420
- Geballe, T. R., Rigaut, F., Roy, J.-R., & Draine, B. T. 2004, *ApJ*, 602, 770
- Genzel, R., Schödel, R., Ott, T., Eisenhauer, F., Hofmann, R., & Lehnert, M. 2003, *ApJ*, 594, 812
- Hanson, M. M., Conti, P. S., & Rieke, M. J. 1996, *ApJS*, 107, 281
- Hanson, M. M., Kudritzki, R.-P., Kenworthy, M. A., Puls, J., & Tokunaga, A. T. 2005, *ApJS*, 161, 154
- Herrero, A., Puls, J. & Najarro, F., 2002, *A&A*, 396, 949
- Hillier, D.J. & Miller, D.L. 1998, *ApJ*, 496, 407
- Hillier, D.J. & Miller, D.L. 1999, *ApJ*, 519, 354
- Maeder, A. & Meynet, G. 2003, *A&A*, 404, 975
- Lacy, J.H., Achtermann, J.M. & Serabyn, E. 1991, *ApJ*, 380, L71
- Lacy, J. H., Townes, C. H., Geballe, T. R., & Hollenbach, D. J. 1980, *ApJ*, 241, 132
- Lenorzer, A., Mokiem, M. R., de Koter, A., & Puls, J. 2004, *A&A* 422, 275
- Najarro, F. 1995, PhD Thesis, Ludwig-Maximilian University, Munich
- Najarro, F., Figer, D. F., Hillier, D.J. & Kudritzki, R.P., 2004, *ApJ*, 611, L105
- Najarro, F., et al. 2006, *A&A*, in press (astro-ph 0605211)
- Paumard, T., et al. 2006, *ApJ*, in press (astro-ph 0601268)

- Repolust, T., Hanson, M. M., Kudritzki, R.-P., & Mokiem, M. R. 2005, *A&A*, 240, 261
- Rigaut, F., Geballe, T. R., Roy, J.-R., & Draine, B. T., 2003, in *Galactic Center Workshop 2002: The Central 300 Parsecs of the Milky Way*, ed. A. Cotera et al., *Astron. Nachr.*, 324, S1, 551
- Scoville, N. Z., Stolovy, S. R., Rieke, M., Christopher, M., & Yusef-Zadeh, F. 2003, *ApJ*, 594, 294
- Tanner, A., Ghez, A.M., Morris, M., Becklin, E.E., Cotera, A., Ressler, M., Werner, M. & Wizinowich, P. 2002, *ApJ*, 575, 860
- Tanner, A., Ghez, A. M., Morris, M. R., & Christou, J. C. 2005, *ApJ*, 624, 742
- Tanner, A., et al. 2006, *ApJ*, in press (astro-ph 0510028)
- Wallace, L. & Hinkle, K. 1997, *ApJS*, 111, 445
- Wellstein, S. & Langer, N., 1999, *A&A*, 350, 148

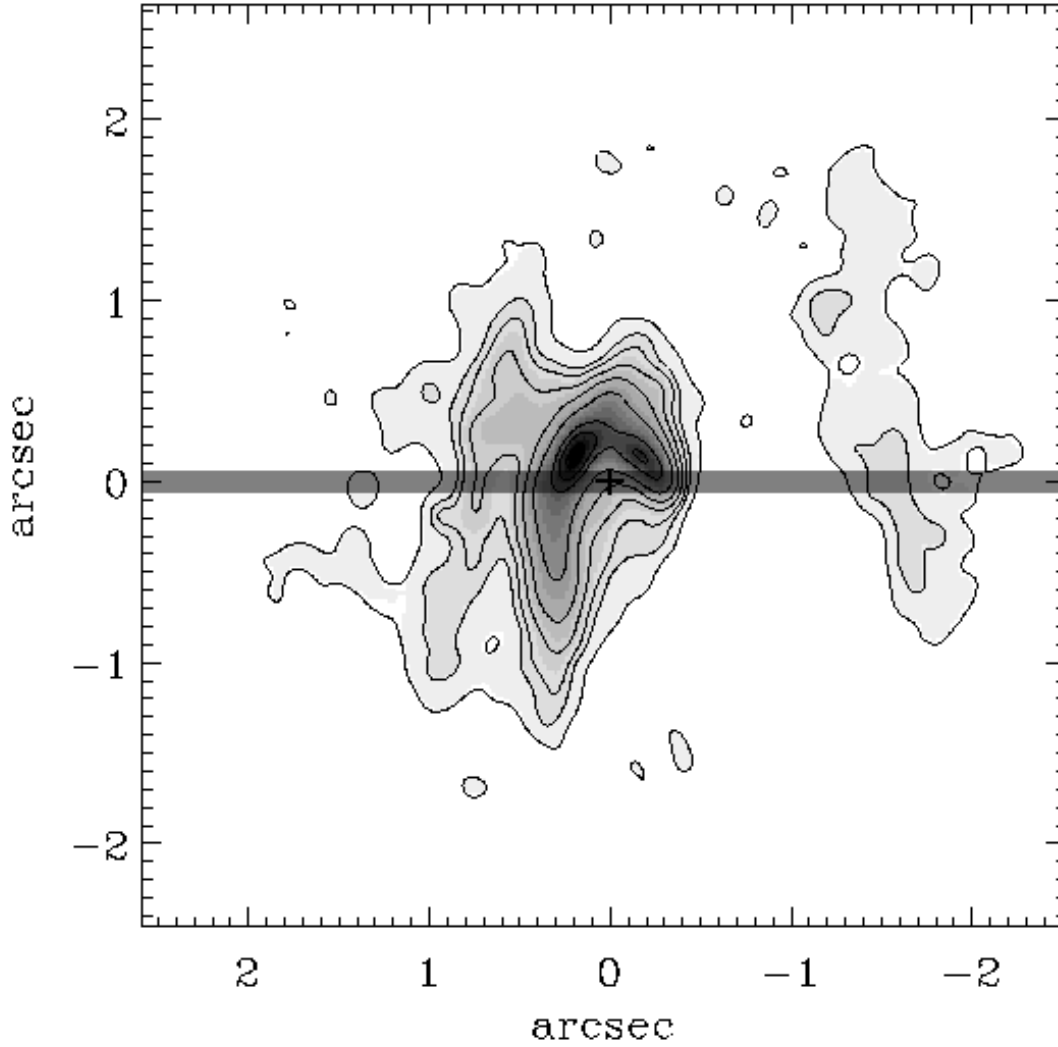


Fig. 1.— Contour plot of the IRS 8 region obtained through a narrow band $2.3 \mu\text{m}$ filter, with the point sources removed, from Geballe et al. (2004). The cross indicates the location of the central star of IRS 8. North is up; east is to the left. The location of the slit used to obtain the spectra presented here is denoted by the narrow shaded rectangle.

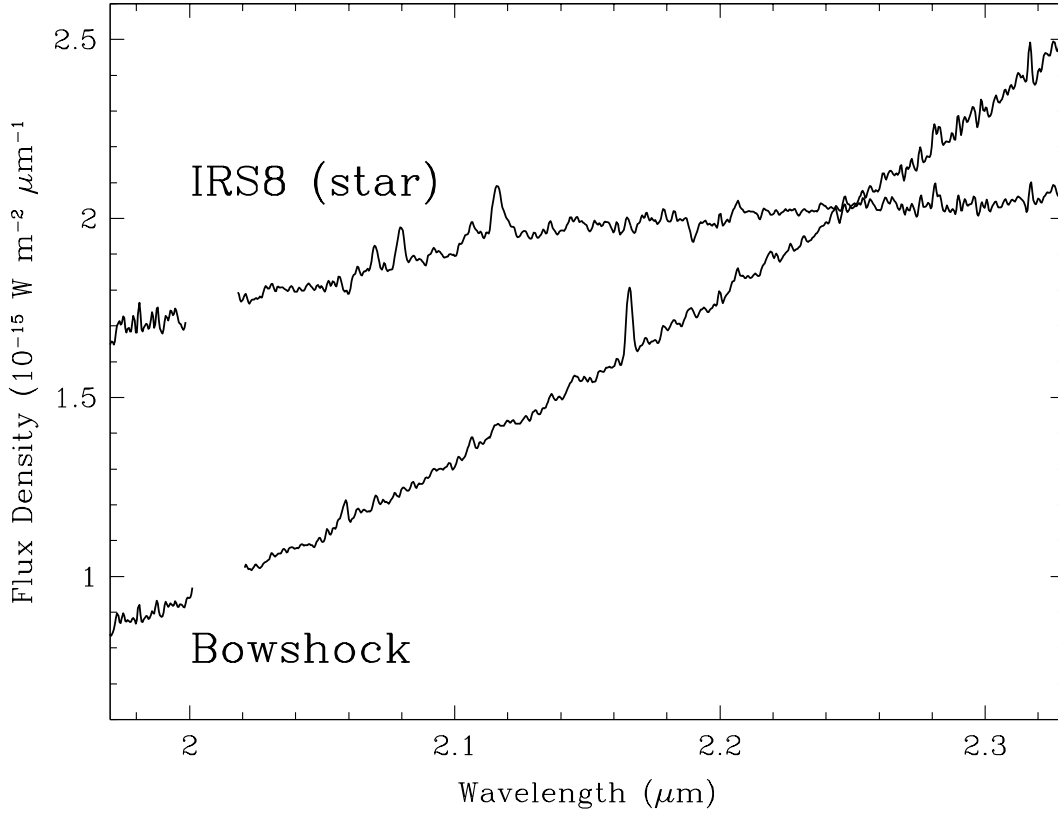


Fig. 2.— Spectra of the central star of IRS 8 and of a $0.10'' \times 0.15''$ (NS \times EW) portion of the bowshock centered $0.24''$ east of the central star.

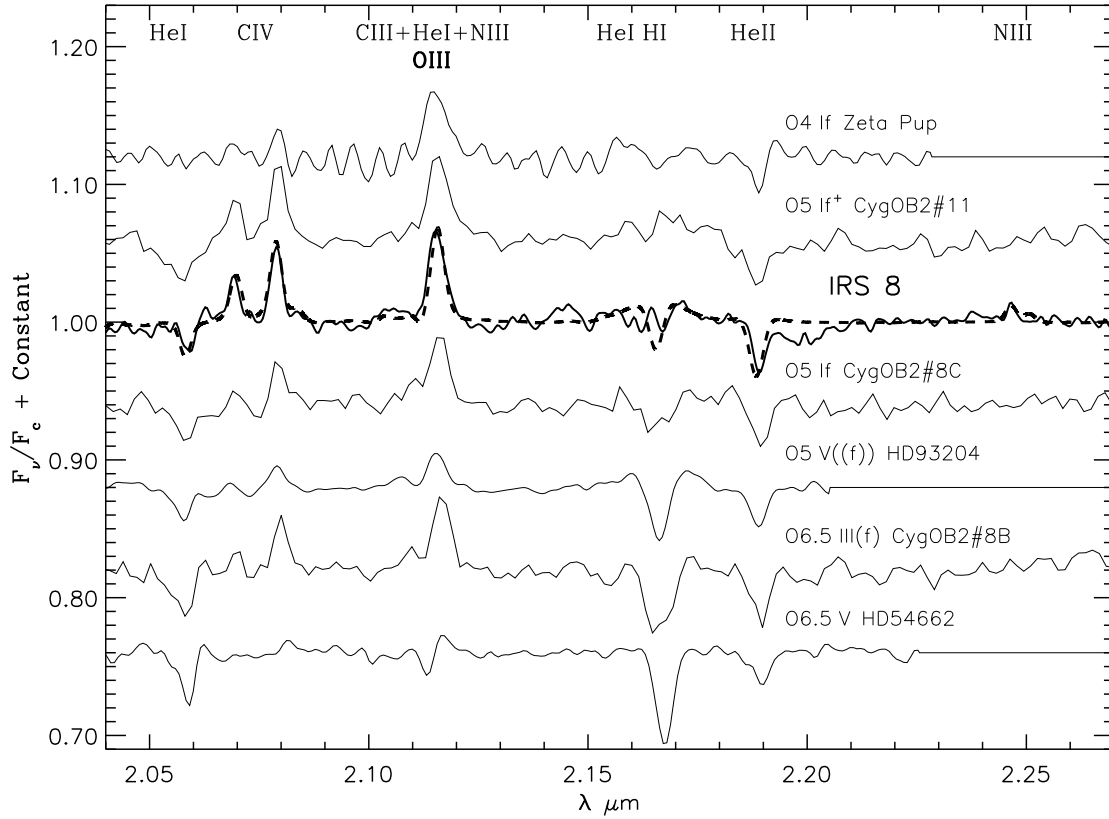


Fig. 3.— Spectral type determination of IRS 8*. Comparison of the resulting normalized spectrum with K-band spectra from Hanson, Conti, & Rieke (1996). degraded to a resolution of $R=800$. Also displayed (dashed) is a model fit with stellar parameters corresponding to an O5.5If star (see text). Wavelengths of important emission and absorption lines are roughly indicated by labels at top of figure

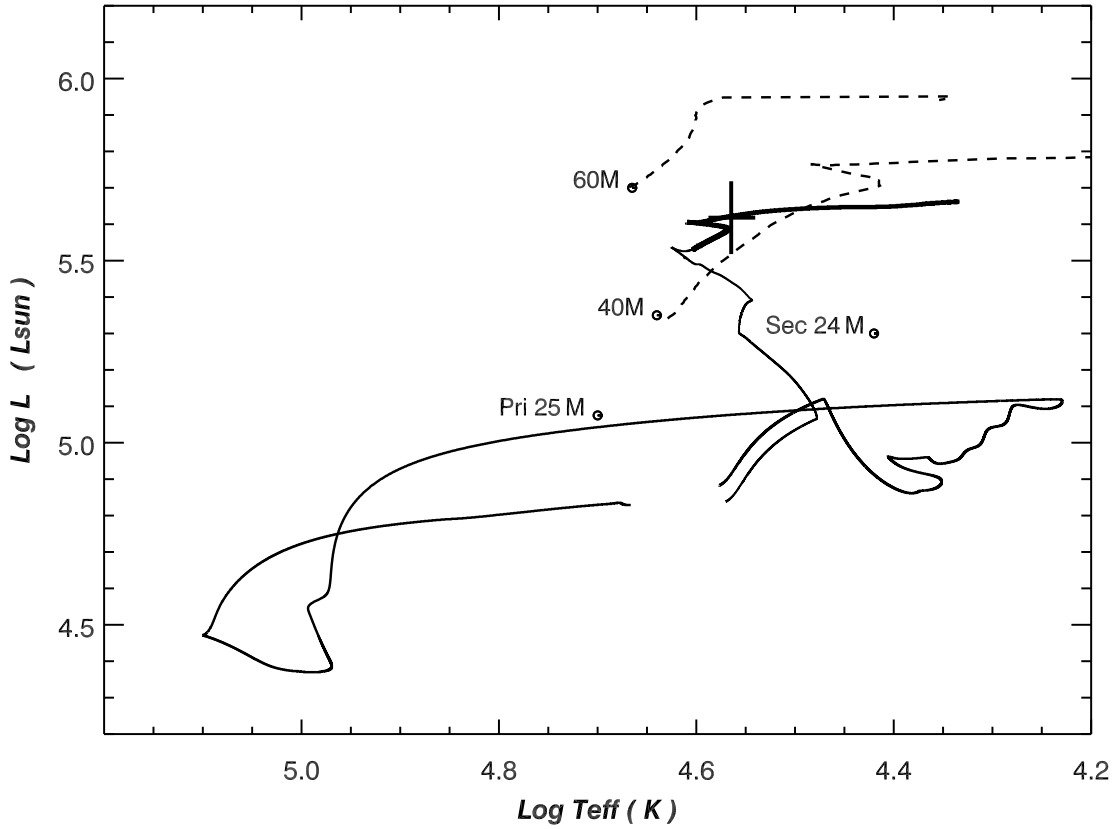


Fig. 4.— Position of IRS 8* (solid cross) in the HR diagram as estimated from model fits, compared with different evolutionary scenarios. Dashed curves correspond to models for 60 and 40 M_{\odot} single stars including rotation Maeder & Meynet (2003) during the pre-WN phase. Solid curves correspond to the evolution of the primary and secondary components of a massive close binary system with initial masses of 25 and 24 M_{\odot} Wellstein & Langer (1999), their model 10a. The thick solid line displayed on the track of the secondary corresponds to the phase where the primary is at least 10 times less bright at K than the secondary. The current location of IRS 8* is reached after 3.6 and 7.1 million years for the single star and massive close binary evolutionary cases respectively (see discussion in text).